

Thermally activated energy and flux flow Hall effect of $\text{Fe}_{1+y}(\text{Te}_{1-x}\text{S}_x)_z$

Hechang Lei,¹ Rongwei Hu,^{1,*} E. S. Choi,² and C. Petrovic¹

¹*Condensed Matter Physics and Materials Science Department,
Brookhaven National Laboratory, Upton, NY 11973, USA and*

²*NHMFL/Physics, Florida State University, Tallahassee, Florida 32310, USA*

(Dated: November 16, 2018)

Thermally activated flux flow (TAFF) and flux flow Hall effect (FFHE) of $\text{Fe}(\text{Te},\text{S})$ single crystal in the mixed state are studied in magnetic fields up to 35 T. Thermally activated energy (TAE) is analyzed using conventional Arrhenius relation and modified TAFF theory which is closer to experimental results. The results indicate that there is a crossover from single-vortex pinning region to collective creep pinning region with increasing magnetic field. The temperature dependence of TAE is different for $H//ab$ and $H//c$. On the other hand, the analysis of FFHE in the mixed state indicates that there is no Hall sign reversal. We also observe scaling behavior $|\rho_{xy}(H)| = A\rho_{xx}(H)^\beta$.

PACS numbers: 74.25.Wx, 74.25.F-, 74.25.Op, 74.70.Dd

I. INTRODUCTION

The discovery of iron based materials has generated enormous interests in the field of superconductivity.^{1–6} Due to similar layered structure to cuprate oxides and rather high T_c , iron based superconductors could host rich vortex phenomena in the mixed state.^{7–10} Recent work suggests that vortex properties of iron based materials seem to be similar to the cuprate superconductors since magnetic flux collective pinning and creep region as well as fishtail effects (second peak effect) have been observed in LnOFeAs ($\text{Ln}=\text{rare earth elements}$, 1111 system) and AFe_2As_2 ($\text{A}=\text{alkaline earth elements}$, 122 system).^{11–14}

Iron based superconductors, $\text{FeSe}_{1-x}\text{Te}_x$, $\text{Fe}_{1+y}\text{Te}_{1-x}\text{Se}_x$, and $\text{Fe}_{1+y}\text{Te}_{1-x}\text{S}_x$ (11 system),^{6,15–21} are of interest both for the technological applications and for the understanding of the vortex properties in the mixed state due to rather simple structure and nearly isotropic upper critical field.^{22–24} Only a limited amount of information on the vortex behavior in single crystals of 11 system is available until now, mainly focusing on thermally activated flux flow (TAFF) region in $\text{Fe}(\text{Te},\text{Se})$.^{25,26} Normal carriers in the vortex core, which experience a Lorentz force, can lead to normal Hall effect in mixed state. On the other hand, flux flow can also induce Hall effect in the mixed state. In detail, when applying a transport current, the flux lines will experience the Lorentz force, $\mathbf{F} = \frac{1}{c}\mathbf{j} \times \mathbf{B}$, where \mathbf{j} is the supercurrent density and \mathbf{B} is the magnitude of magnetic induction. The motion of magnetic flux lines produces a macroscopic electric field \mathbf{E} which is given by $\mathbf{E} = -\frac{1}{c}\mathbf{v} \times \mathbf{B}$, where \mathbf{v} is the velocity of vortex motion.²⁷ The vortex motion along the Lorentz force (perpendicular to \mathbf{j}) gives the dissipative field ($\mathbf{E}||\mathbf{j}$) and generates the flux flow resistivity, whereas the vortex motion along the direction of supercurrent results in the Hall electric field ($\mathbf{E}\perp\mathbf{j}$). Therefore the flux flow Hall effect (FFHE) is a sensitive method to study the vortex dynamics.

There are two exotic phenomena in connection with FFHE in cuprate superconductors. One is a sign reversal

of the Hall resistivity $\rho_{xy}(H)$ below T_c .²⁸ This anomaly has also been observed in some conventional superconductors, e.g. amorphous MoSi_3 ,²⁹ and 2H-NbSe_2 .³⁰ The sign change is not expected within the classical Bardeen-Stephen³¹ and Nozières-Vinen³² theories of vortex motion, which predict that the Hall sign in the superconducting and normal state should be the same. Several models have been proposed for interpreting this anomaly,^{33–36} however its origin remains a controversy. Another phenomenon is a scaling law between $\rho_{xy}(H)$ and the longitudinal resistivity $\rho_{xx}(H)$ in the superconducting transition region, i.e., $|\rho_{xy}(H)| = A\rho_{xx}(H)^\beta$ with different values of β for different materials.^{37,38}

In this paper, we study the vortex properties of $\text{Fe}_{1.14(1)}(\text{Te}_{0.91(2)}\text{S}_{0.09(2)})_z$ single crystal via TAFF resistivity and FFHE in the mixed state. The temperature dependence of TAE is different for $H//ab$ and $H//c$. Furthermore, there is a crossover from single-vortex pinning region to collective creep pinning region with increasing magnetic field. On the other hand, there is no sign reversal and we observe scaling behavior for FFHE.

II. EXPERIMENT

Single crystals of $\text{Fe}(\text{Te},\text{S})$ were grown by self flux method and their crystal structure was analyzed in the previous report.²³ The elemental analysis of the crystal used in this study showed the stoichiometry is $\text{Fe}:\text{Te}:\text{S}=1.14(1):0.91(1):0.09(2)$ and we denote it as S-09 in the following for brevity. Electrical transport measurements were performed using a four-probe configuration with current flowing in the ab -plane of tetragonal structure in dc magnetic fields up to 9 T in a Quantum Design PPMS-9 from 1.9 to 200 K and up to 35 T in a He3 cryostat system with resistive magnet down to 0.3 K at the National High Magnetic Field Laboratory (NHMFL) in Tallahassee, FL. Hall contacts with typical misalignment of less than 0.1 mm were used. At each point the Hall voltage was measured for two directions of the magnetic field, which is always perpendicular to current direction.

III. RESULTS AND DISCUSSIONS

Fig. 1(a,b) show the resistivity $\rho(T, H)$ of S-09 near the superconducting transition region for $H \parallel ab$ plane and $H \parallel c$ axis. With increasing magnetic fields, the resistivity transition widths are broadened gradually. The onset of superconductivity shifts to lower temperatures for both magnetic field directions, but the trend is more obvious for $H \parallel c$ than $H \parallel ab$. According to the TAFF theory, the resistivity in TAFF region can be expressed as,^{7,9,39}

$$\rho = (2\nu_0 LB/J) \exp(-J_{c0} BVL/T) \sinh(JBVL/T) \quad (1)$$

where ν_0 is an attempt frequency for a flux bundle hopping, L is the hopping distance, B is the magnetic induction, J is the applied current density, J_{c0} is the critical current density in the absence of flux creep, V is the bundle volume and T is the temperature. If J is small enough and $JBVL/T \ll 1$, we obtain

$$\rho = (2\rho_c U/T) \exp(-U/T) = \rho_{0f} \exp(-U/T) \quad (2)$$

where $U = J_{c0} BVL$ is the thermally activated energy (TAE) and $\rho_c = \nu_0 LB/J_{c0}$, which is usually considered to be temperature-independent. For cuprate superconductors, the prefactor $2\rho_c U/T$ is usually assumed as a constant ρ_{0f} ,⁹ therefore, $\ln \rho(T, H) = \ln \rho_{0f} - U(T, H)/T$, where H is the external magnetic field. On the other hand, according to the condensation model,³⁹ $U(T, H) = H_c^2(t)\xi^n(t)$, where H_c is the thermal critical field, ξ is the coherence length, $t = T/T_c$ (T_c is the superconducting transition temperature), and n depends on the dimensionality of the vortex system with the range from 0 to 3. Since $H_c \propto 1 - t$, and $\xi \propto (1 - t)^{-1/2}$ near T_c ,⁴⁰ it is obtained that $U(T, H) = U_0(H)(1 - t)^q$, where $q = 2 - n/2$. It is generally assumed that $U(T, H) = U_0(H)(1 - t)$, i.e. $n = 2$, and the $\ln \rho - 1/T$ becomes Arrhenius relation, $\ln \rho(T, H) = \ln \rho_0(H) - U_0(H)/T$, where $\ln \rho_0(H) = \ln \rho_{0f} + U_0(H)/T_c$ and $U_0(H)$ is the apparent activation energy. Furthermore, it can be concluded that $-\partial \ln \rho(T, H) / \partial T^{-1} = U_0(H)$. Hence, the $\ln \rho$ vs. $1/T$ should be linear in TAFF region. The slope is $U_0(H)$ and its y-intercept represents $\ln \rho_0(H)$.

In the Figs. 1(a,b), the solid lines show the Arrhenius relation in TAFF region. Note that the results are shown in the common logarithmic scale in the figures, but we calculate them in the natural one. All linear fits intersect at approximately the same point T_{cross} , which is about 8.63 and 8.34 K for $H \parallel ab$ and $H \parallel c$, respectively. Assuming the temperature dependences of $\rho_{ab}(T, H)$ at two different magnetic fields (H_1 and H_2) can be fitted by Arrhenius relation, according to above discussion, we get $\ln \rho(T, H_1) = \ln \rho_{0f} + U_0(H_1)/T_c - U_0(H_1)/T$ and $\ln \rho(T, H_2) = \ln \rho_{0f} + U_0(H_2)/T_c - U_0(H_2)/T$. When $\rho(T, H_1) = \rho(T, H_2)$, it can be obtained $T = T_c$, therefore, ideally, all the lines at different fields should be crossed into same point, T_{cross} , which is equal to T_c . According to the conventional analysis, the $\ln \rho_{0f}$ and T_c

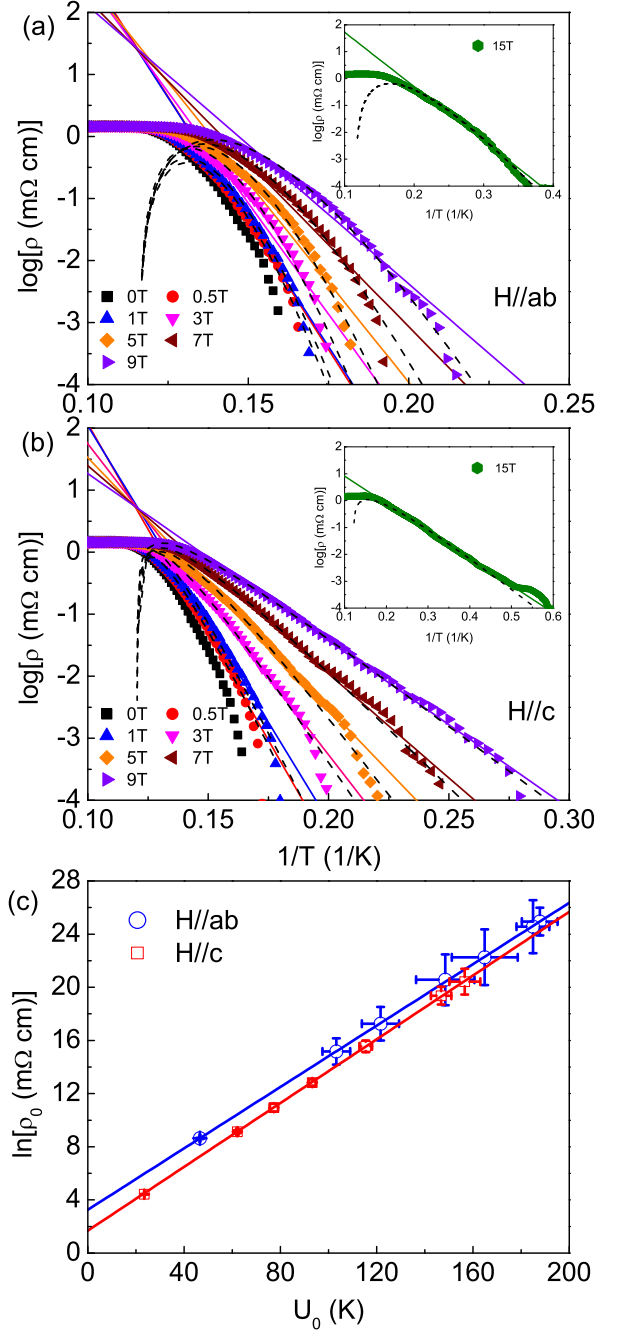


FIG. 1. (a) and (b) Longitudinal resistivities $\rho(T, H)$ of S-09 in different magnetic field directions for $H \parallel ab$ and $H \parallel c$ below 10K, respectively. The corresponding solid and black dashed lines are fitting results from the Arrhenius relation and eq. (3). (c) $\ln \rho_0$ vs U_0 derived from Arrhenius relation for $H \parallel ab$ and $H \parallel c$.

can be obtained from linear fits $\ln \rho_0(H)$ and $U_0(H)$ using $\ln \rho_0(H) = \ln \rho_{0f} + U_0(H)/T_c$ (shown in Fig. 1(c)). From the fitting results, values of ρ_{0f} and T_c are $27.22 \pm 4.77 \text{ m}\Omega \cdot \text{cm}$, $8.72 \pm 0.82 \text{ K}$ and $5.23 \pm 1.42 \text{ m}\Omega \cdot \text{cm}$, $8.32 \pm 0.48 \text{ K}$ for $H \parallel ab$ and $H \parallel c$, respectively. The T_c is consistent with the values of T_{cross} in the range of errors. It seems that the $\rho(T, H)$ can be fitted with straight lines

well. However, close inspection shows that there is rather large fitting errors, especially for $H \parallel ab$. The origin of the large errors is the Arrhenius relation that can only be satisfied in the limited region and this region is narrower for $H \parallel ab$. The effects of prefactor and non-linear relation of $U(T, H)$ lead to $\rho(T, H)$ deviating from Arrhenius relation (vide infra).

Fig. 2(a,b) shows the temperature dependence of $-\partial \ln \rho(T, H) / \partial T^{-1}$ for both field directions. Because the assumptions $U(T, H) = U_0(H)(1 - t)$ and $\rho_{0f} = \text{const}$ lead to $-\partial \ln \rho(T, H) / \partial T^{-1} = U_0(H)$, $U_0(H)$ should be a set of horizontal lines. We present this in Fig. 2(a,b) over a limited length. Each length covers the temperature interval used for estimating $U_0(H)$ in the Arrhenius relation. It can be seen that $-\partial \ln \rho(T, H) / \partial T^{-1}$ increases sharply with decreasing temperature, which was also observed in Bi-2212 thin films.⁴¹ The center of each $U_0(H)$ horizontal line approximately intersects $-\partial \ln \rho(T, H) / \partial T^{-1}$ curve and the overlapping region is increasing with temperature decrease. This shows that each $U_0(H)$ is only the average value of its $-\partial \ln \rho(T, H) / \partial T^{-1}$ in the fitting temperature region. Hence, the TAE determined from the conventional method does not reflect the true evolution of $U(T, H)$ with the temperature, particularly for $H \parallel ab$. This contradiction originates from two basic assumptions introduced for Arrhenius relation: one is the constant prefactor $\rho_{0f} = 2\rho_c U/T$ and another is the linear relation $U(T, H) = U_0(H)(1 - t)$. Zhang *et al*⁴² suggested that the temperature-dependent prefactor and nonlinear relation of $U(T, H) - T$ should be considered. In the following section, we will analyze the resistivity results using this more general method.⁴²

Using the relation $U(T, H) = U_0(H)(1 - t)^q$, from eq. (2) it can be derived that

$$\ln \rho = \ln(2\rho_c U_0) + q \ln(1 - t) - \ln T - U_0(1 - t)^q / T \quad (3)$$

and

$$-\partial \ln \rho / \partial T^{-1} = [U_0(1 - t)^q - T][1 + qt / (1 - t)] \quad (4)$$

where ρ_c and U_0 are temperature independent and T_c derived from Arrhenius relation is used for fitting. Therefore, there are three free parameters, q , ρ_c and U_0 in eq. (3). The fitting results are shown in Fig. 1. From Fig. 1(a,b), it can be seen that all fits are in good agreement with experimental data and the results are better than Arrhenius relation. This is more pronounced for $H \parallel ab$. Fig. 2(a,b) clearly shows the advantage of eq. (3) over Arrhenius relation. The TAFF formula (eq. (1)) can effectively capture the upturn trend of $-\partial \ln \rho / \partial T^{-1}$ with decreasing temperature when the (linear or nonlinear) correlations between prefactor as well as $U(T, H)$ and T are considered. In detail, when $T \ll U$ (corresponding to $T \ll U_0(1 - t)^q$), it can be derived that $-\partial \ln \rho / \partial T^{-1} = U_0(1 - t)^q [1 + qt / (1 - t)]$ and when $q = 1$, $-\partial \ln \rho / \partial T^{-1} = U_0$, i.e. Arrhenius relation. Because the

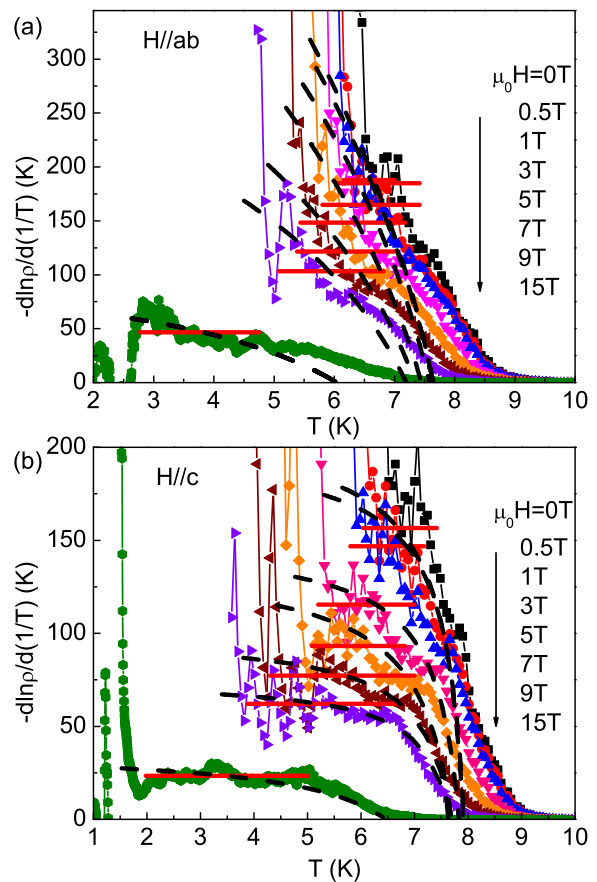


FIG. 2. Experimental $-\partial \ln \rho / \partial T^{-1}$ data in TAFF region for $H \parallel ab$ (a) and $H \parallel c$ (b), respectively. The red solid horizontal lines correspond to obtained $U_0(H)$ from Arrhenius relation and the blue dashed lines are plotted using eq. (4). The parameters are determined via fitting eq. (3) to corresponding experimental resistivity data shown in Fig.1 (a) and (b).

obtained U_0 of S-09 is much smaller than that of cuprates superconductors (shown in Fig. 3) and it is comparable with temperature, the assumption $T \ll U$ can not be satisfied and the temperature dependence of prefactor should be considered.

Fig. 3 presents the $U_0(H)$ and $q(H)$ obtained from experimental data fits using eq. (3) at different fields. The $U_0(H)$ shows a power law ($U_0(H) \sim H^{-\alpha}$) field dependence for both directions. For $H \parallel ab$, $\alpha = 0.12 \pm 0.02$ for $\mu_0 H < 5T$ and $\alpha = 1.70 \pm 0.30$ for $\mu_0 H > 5T$; For $H \parallel c$, $\alpha = 0.21 \pm 0.03$ for $\mu_0 H < 5T$ and $\alpha = 1.34 \pm 0.16$ for $\mu_0 H > 5T$. The weak field dependence of $U_0(H)$ in low field for both orientations suggests that single-vortex pinning dominates in this region.⁷ The vortex spacing becomes significantly smaller than penetration depth in higher fields and we expect a crossover to a collective-pinning regime where the activation energy becomes strongly dependent on the field, i.e., the collective creep dominance.⁴³ Because α is larger than 1 at this regime, it is possible that the flux lines are pinned by the collective point defects in the high field region.⁴⁴ Similar crossover has been observed in Nd(O,F)FeAs single

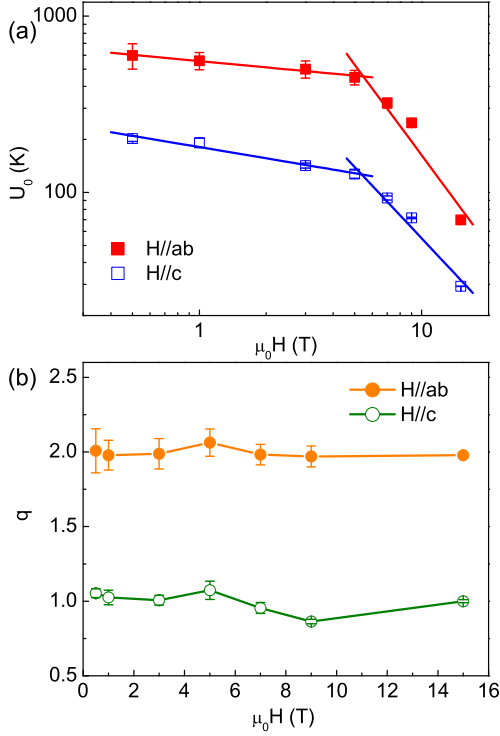


FIG. 3. (a) U_0 and (b) q as functions of magnetic fields obtained from fitting the resistivity in TAFF region using eq. (3). The opened and filled squares represent U_0 for $H//c$ and $H//ab$, respectively, while the opened and filled circles show corresponding q , respectively. The solid lines in (a) are power-law fitting using $U_0(H) \sim H^{-\alpha}$.

crystal.⁴⁵ The values of q change from about 1 for $H//c$ to 2 for $H//ab$, independent on the intensity of field for both directions. The value of $q = 2$ has also been observed in many cuprates superconductors.^{41,42,46}

It should be noted that although the Fe(Te,S) sample has low volume fraction, it should not have obvious effect on the analysis of TAFF. Due to the inhomogeneity of sample, the conductivity of sample can be expressed as $\sigma = \sigma_{sc} + \sigma_{normal}$, where σ_{sc} is the conductivity in superconducting state and σ_{normal} is the conductivity of normal state. When $T < T_{c,zero}$, σ_{sc} is infinite and thus $\sigma = \sigma_{sc} = \infty$, i.e., $\rho = 0$ and the normal state part of sample is short-circuited. On the other hand, the resistivity in the TAFF regime is about one to three orders of magnitude less than normal state^{9,39}. It means that although the conductivity σ_{sc} in this range is finite, it is still much larger than σ_{normal} , and we can obtain $\sigma \approx \sigma_{sc}$.

The Hall effect in the mixed state gives important insight in the flux flow. In the following section, we will discuss the vortex dynamics of S-09 in flux flow region. The field dependence of the longitudinal resistivity $\rho_{xx}(H)$ for $H//c$ is shown in Fig. 4(a). Superconductivity is suppressed by increasing magnetic field up to 35 T and the transition of $\rho_{xx}(H)$ are shifted to lower magnetic fields at higher temperature. At the lowest measuring

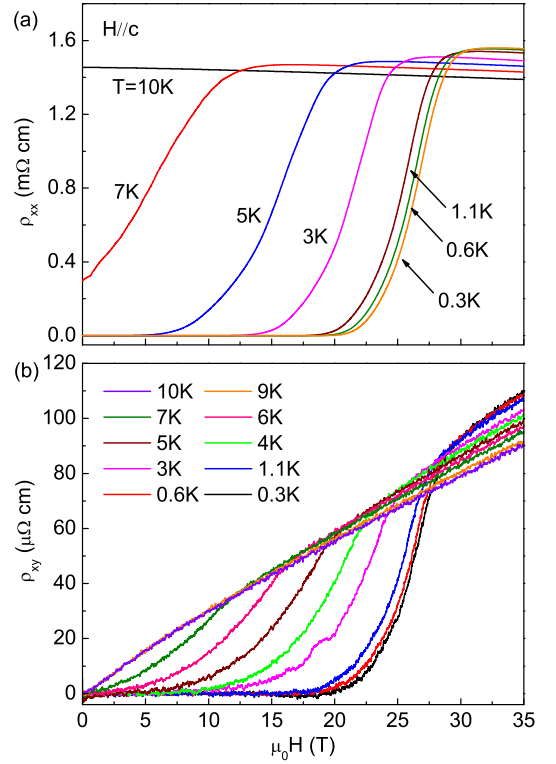


FIG. 4. Field dependence of (a) Longitudinal resistivity $\rho_{xx}(H)$ and (b) Hall resistivity $\rho_{xy}(H)$ at various temperatures in dc magnetic fields up to 35T for $H//c$.

temperature ($T = 0.3K$), normal state is recovered from superconducting state when field is up to 30 T. Fig. 4(b) shows the Hall resistivity at $T \leq 10K$. It can be seen that $\rho_{xy}(H) = 0$ in low field when temperature is below T_c . At higher field region close to the superconducting transition, the absolute values of Hall resistivity increase and gradually reach the $\rho_{xy}(H)$ curve obtained in the normal state at temperatures slightly higher than T_c . The $\rho_{xy}(H)$ in the mixed state shifts with increasing temperature to lower fields. All of these features are similar to the $\rho_{xx}(H)$ results. On the other hand, the normal state $\rho_{xy}(H)$ curves are very close to linear, except for low field parts where there is slight nonlinearity with negative curvatures that can be ascribed to skew scattering due to excess Fe.⁴⁷

The sign of the Hall resistivity is positive in the mixed state as well as in the normal state indicating hole type carriers. There is no sign reversal for $\rho_{xy}(H)$ in the mixed state, which is a typical behavior for hole- and electron-type cuprate superconductors below T_c .^{28,48} Because Hall conductivity $\sigma_{xy}(H) [= \rho_{xy}(H)/(\rho_{xx}(H)^2 + \rho_{xy}(H)^2) \cong \rho_{xy}(H)/\rho_{xx}(H)^2$, when $\rho_{xx}(H) \gg |\rho_{xy}(H)|$] is usually insensitive to disorder by a general argument of the vortex dynamics, it is convenient to discuss the Hall results using $\sigma_{xy}(H)$.^{38,49} There are two contributions to the $\sigma_{xy}(H)$ in the mixed state:

$$\sigma_{xy}(H) = \sigma_{xy,n}(H) + \sigma_{xy,sc}(H) \quad (5)$$

where $\sigma_{xy,n}(H)$ is the conductivity of normal quasiparticles that experience a Lorentz force inside and around the vortex core. This term has the same sign as the normal state and is proportional to H . The second term $\sigma_{xy,sc}(H)$ is an anomalous contribution due to the motion of vortices parallel to the electrical current density \mathbf{j} .

From the theory based on the time-dependent Ginzburg-Landau (TDGL) equation, $\sigma_{xy,sc}(H) \propto 1/H$ and it could have a sign opposite to that of $\sigma_{xy,n}(H)$.^{33,34} Furthermore, the $\sigma_{xy,sc}(H)$ is the dominant term at low field but at higher field $\sigma_{xy,n}(H)$ are important and could dominate over $\sigma_{xy,sc}(H)$. Therefore, if $\sigma_{xy,sc}(H)$ has a different sign when compared to $\sigma_{xy,n}(H)$, it is possible to observe a sign reversal in the Hall effect in the superconducting state,^{33,34} as for example in YBCO.⁵⁰ On the other hand, it can be easily seen in Fig. 5(a) that the Hall conductivity decreases with increasing field and the field dependence of $\sigma_{xy}(H)$ changes more rapidly than $1/H$. This suggests that $\sigma_{xy}(H)$ is not independent of disorder in the strong pinning regime.⁵¹ According to the theory proposed by Fukuyama, Ebisawa, and Tsuzuki (FET),⁵² the sign of $\sigma_{xy,sc}(H)$ is given by the sign of $sgn(e)\partial N(\mu)/\partial\mu|_{\mu=E_F}$, where $sgn(e)$ is the sign of the carrier, $N(\mu)$ is the density of states, μ is the chemical potential, and E_F is the Fermi energy. On the other hand, in the phenomenological theory based on Ginsburg-Landau equation and its gauge invariance,³⁵ the sign of the $\sigma_{xy,sc}(H)$ is determined by the signs of $sgn(e)\partial\ln T_c/\partial\mu$. In any case, the sign of the Hall effect in the mixed state depends on the details of the band structure. For a complicated Fermi surface, the signs of $\sigma_{xy,sc}(H)$ may be different from that of $\sigma_{xy,n}(H)$. Therefore, contrary to cuprate superconductors, the difference of Fermi surface may be one origin of absence of sign reversal in Fe(Te,S). On the other hand, cuprate superconductors are d-wave superconductors, whereas, for Fe(Te,S), the gap function is unknown, but is most likely s-wave. This difference could be another origin of different contribution of the vortex cores to the Hall conductivity.⁵³

At high magnetic fields, we observe $|\rho_{xy}(H)| = A\rho_{xx}(H)^\beta$ scaling (Fig. 4(b)). The values of β are in the range of 0.9 – 1.0 and increase slightly with temperature. A phenomenological model considering the effect of pinning on the Hall resistivity proposed by Vinokur et al.,⁴⁹ gives the scaling index $\beta = 2$ which, as well as Hall conductivity, is independent on the degree of disorder. This is believed to be a general feature of any vortex state with disorder dominated dynamics. On the other hand, based on the normal core model proposed by Bardeen and Stephen,³¹ Wang, Dong, and Ting (WDT),^{54,55} developed a theory for the Hall effect that includes both pinning and thermal fluctuations. In the WDT theory the scaling behavior is explained by taking into account the backflow current of vortices due to pinning. Thereby β changes from 2 to 1.5 as the pinning strength increases.⁵⁵ This has been observed in irradiated YBCO

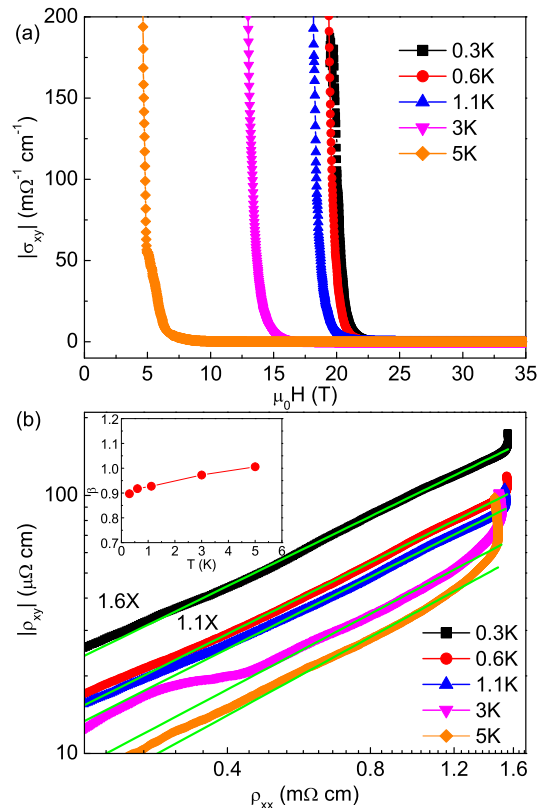


FIG. 5. (a) Field dependence of absolute values of the Hall conductivity $|\sigma_{xy}(H)|$ measured at various temperatures in dc magnetic fields up to 35T. (b) $|\rho_{xy}|$ vs ρ_{xx} at various temperatures. The solid lines are fitting results using the scaling behavior $|\rho_{xy}(H)| = A\rho_{xx}(H)^\beta$. Inset of (b) shows the temperature dependence of $\beta(T)$.

samples, where β was found to decrease from 1.5 compared to 2 after irradiation,⁵⁶ and in $\text{HgBa}_2\text{CaCu}_2\text{O}_{6+x}$ thin films with columnar defects, where β changes from 1.0 to 1.2 with increasing the field.⁵⁷ Therefore, small values of β in S-09 (inset of Fig. 4(b)) may be connected with the strong pinning strength due to the considerably large concentration of defects in $\text{Fe}_{1+y}(\text{Te}_{1-x}\text{S}_x)_z$.²³

IV. CONCLUSION

In summary, we investigated the resistive TAFF and flux flow Hall effect of $\text{Fe}_{1.14(1)}(\text{Te}_{0.91(2)}\text{S}_{0.09(2)})_z$ single crystal in high and stable magnetic fields up to 35 T. TAFF behavior could be understood within the framework of modified Arrhenius relation assuming that the prefactor ρ_{0f} is temperature-dependent while ρ_c is temperature-independent, and $U(T, H) = U_0(H)(1-t)^q$, q can be set as a free parameter for fitting not limited to 1. There is a crossover from single-vortex pinning region to collective creep region for both field direction. Furthermore, q changes from 1 to 2 when magnetic field is rotated along ab plane to c axis but it is not sensitive to the magnitude of magnetic field below

- Lett. **74**, 2351 (1995).
- ³⁹ T. T. M. Palstra, B. Batlogg, R. B. van Dover, I. F. Schneemeyer, and J. V. Waszczak, Phys. Rev. B **41**, 6621 (1990).
- ⁴⁰ E. H. Brandt, Rep. Prog. Phys. **58**, 1465 (1995).
- ⁴¹ Y. Z. Zhang, Z. Wang, X. F. Lu, H. H. Wen, J. F. de Marneffe, R. Deltour, A. G. M. Jansen, and P. Wyder, Phys. Rev. B **71**, 052502 (2005).
- ⁴² Y. Z. Zhang, H. H. Wen, and Z. Wang, Phys. Rev. B **74**, 144521 (2006).
- ⁴³ Y. Yeshurun and A. P. Malozemoff, Phys. Rev. Lett. **60**, 2202 (1988).
- ⁴⁴ C. C. Chin and T. Morishita, Physica C **207**, 37 (1993).
- ⁴⁵ J. Jaroszynski, F. Hunte, L. Balicas, Y.-J. Jo, I. Raičević, A. Gurevich, D. C. Larbalestier, F. F. Balakirev, L. Fang, P. Cheng, Y. Jia, and H. H. Wen, Phys. Rev. B **78**, 174523 (2008).
- ⁴⁶ Z. H. Wang and X. W. Cao, Solid State Commun. **109**, 709 (1999).
- ⁴⁷ H. C. Lei, R. W. Hu, E. S. Choi, J. B. Warren, and C. Petrovic, Phys. Rev. B **81**, 184522 (2010).
- ⁴⁸ M. Cagigal, J. Fontcuberta, M. A. Crusellas, J. L. Vicent, and S. Pinol, Physica C **248**, 155 (1995).
- ⁴⁹ V. M. Vinokur, V. B. Geshkenbein, M. V. Feigel'man, and G. Blatter, Phys. Rev. Lett. **71**, 1242 (1993).
- ⁵⁰ D. M. Ginsberg and J. T. Manson, Phys. Rev. B **51**, 515 (1995).
- ⁵¹ Y. Matsuda, T. Nagaoka, G. Suzuki, K. Kumagai, M. Suzuki, M. Machida, M. Sera, M. Hiroi, and N. Kobayashi, Phys. Rev. B **52**, 15749 (1995).
- ⁵² H. Fukuyama, H. Ebisawa, and T. Tsuzuki, Prog. Theor. Phys. **46**, 1028 (1971).
- ⁵³ T. Nagaoka, Y. Matsuda, H. Obara, A. Sawa, T. Terashima, I. Chong, M. Takano, and M. Suzuki, Phys. Rev. Lett. **80**, 3594 (1998).
- ⁵⁴ Z. D. Wang and C. S. Ting, Phys. Rev. Lett. **67**, 3618 (1991).
- ⁵⁵ Z. D. Wang, J. Dong, and C. S. Ting, Phys. Rev. Lett. **72**, 3875 (1994).
- ⁵⁶ W. N. Kang, D. H. Kim, S. Y. Shim, J. H. Park, T. S. Hahn, S. S. Choi, W. C. Lee, J. D. Hettinger, K. E. Gray, and B. Glagola, Phys. Rev. Lett. **76**, 2993 (1996).
- ⁵⁷ W. N. Kang, B. W. Kang, Q. Y. Chen, J. Z. Wu, S. H. Yun, and A. Gapud, J. Z. Qu, W. K. Chu, D. K. Christen, R. Kerchner, and C. W. Chu, Phys. Rev. B **59**, R9031 (1999).